minerals

MDPI

Article

Study on Grinding Behavior Characteristics under Low-Speed Grinding Condition

Shaojian Ma [1,2], Xiaojing Yang [2], Hengjun Li [2], Wenzhe Xu [1], Xingjian Deng [1] and Jinlin Yang [1,*]

[1] Guangxi Higher School Key Laboratory of Minerals Engineering and Materials, College of Resources, Environment and Materials, Guangxi University, Nanning 530004, China
[2] College of Chemistry and Chemical Engineering, Guangxi University, Nanning 530004, China
* Correspondence: jlyang523@126.com; Tel.: +86-131-5266-0958

Abstract: In order to explore the crushing mechanism of minerals, this paper attempts to eliminate the throwing effect of media and study the grinding characteristics of minerals only under the action of abrasion force. In this paper, the method of removing the throwing state of media is to adjust the mill to a lower rotational speed, so that the grinding media are all in a cascading state. Three single-component pure minerals, quartz, pyrrhotite, and pyrite, commonly found in complex ores, were selected as research objects to study the grinding behavior characteristics of the three minerals only under the force of abrasion. The effects of mineral species, feed-particle sizes, grinding time, and other factors on the particle-size distribution and product-generation rate of grinding products are studied. The results show that from the particle-size distribution of grinding products, the yield of coarse particles is the highest, while the yield and t_{10} value of other fine particles are very low. The feed-particle size and the hardness of the mineral sample affect the grinding behavior. The product particle size is mainly 0.71 times the feed-particle size, and the other fine particle sizes generated are less than 0.5 times the feed-particle size.

Keywords: grinding; cascading state; abrasion; pure mineral

Citation: Ma, S.; Yang, X.; Li, H.; Xu, W.; Deng, X.; Yang, J. Study on Grinding Behavior Characteristics under Low-Speed Grinding Condition. *Minerals* **2023**, *13*, 786. https://doi.org/10.3390/min13060786

Academic Editor: Carlos Hoffmann Sampaio

Received: 20 April 2023
Revised: 3 June 2023
Accepted: 6 June 2023
Published: 8 June 2023

1. Introduction

Grinding operations are widely used in solid-resource processing industries such as mining, chemical engineering, metallurgy, and building materials [1–4]. In mineral processing production, grinding plays a very important role. Its basic construction cost accounts for about 60% of the construction cost of the mineral processing plant, and its production cost accounts for 40% to 50% of the mineral processing plant [5]. Grinding is the preparation of material particle size, and its product particle-size distribution will significantly affect the efficiency of subsequent separation operations and the economic and technical indicators of the concentrator [6–8]. Therefore, optimizing grinding operations, improving the grinding process efficiency, and reducing grinding costs are of great significance for the mineral resource processing industry to reduce production costs and improve resource recovery and utilization [9–11].

Ball mills have been widely used in industrial production due to their simple structure, ease of adjustment, reliability, and safety [12–14]. The movement state of the medium inside the ball mill directly affects the grinding power, steel ball consumption, and grinding economic indicators. There are three typical motion states of grinding media, namely, cascade type, throw type, and centrifugal type. For ball-mill media in the throwing state, relevant researchers have conducted a great deal of research [15–19], and relevant theoretical formulas can be used for corresponding quantitative description and analysis. However, the research on grinding in the cascading state only stays at the level of qualitative description [20]. In the cascading state, the abrasion force is the main force to achieve mineral crushing. In the throwing state, the impact force is the main force to

achieve mineral crushing. In fact, the abrasion force is more gentle and uniform than the impact force, so it is more suitable for studying the crushing law of minerals.

In the actual grinding process, the component minerals in multi-component complex ores have different physical, chemical, and mechanical properties, so the ores exhibit different characteristics when subjected to grinding action [21,22]. This is a selective grinding phenomenon of ores. Component minerals with low hardness, high toughness, and many structural defects are more likely to be ground. The difference in the properties of component minerals in ores leads to the interaction between component minerals during the grinding process. This is the negative grinding action of hard minerals on soft minerals and the positive grinding action of soft minerals on hard minerals [23–26].

Therefore, in order to explore the crushing mechanism of different mineral components in ores, this article adjusts the mill to a lower rotational speed, allowing all the grinding media to be in a cascading state. Three single-component pure minerals, quartz, pyrrhotite, and pyrite, commonly found in complex ores, were selected as research objects to study the grinding behavior characteristics of the three minerals only under the force of abrasion. This research further reveal the effects of mineral sample types, feed-particle sizes, grinding time, and other factors on the particle-size distribution and product-generation rate of grinding products.

2. Materials and Methods

2.1. Materials

The samples used in the test are natural quartz, pyrrhotite, and pyrite. Before grinding, the mineral raw materials are crushed to −3.35 mm, and then sieved into three particle sizes: −3.35 + 2.36 mm, −2.36 + 1.7 mm, and −1.7 + 1.18 mm. After mixing, each particle size is evenly divided into 500 g/bag for grinding test. The mill used is a cylindrical ball mill with adjustable rotational speed. The model and specification of the mill are Φ200 mm × 240 mm. The crushing equipment is a jaw crusher, model XPC-100 × 150, and the screening equipment is a vibrating screen, model Analysette 3. The chemical element analysis equipment is an X-ray fluorescence element analyzer, model S8 TIGER. The chemical element analysis results of the three pure minerals are shown in Tables 1–3.

Table 1. Chemical components of quartz.

Component	SiO_2	Fe_2O_3	MgO	Al_2O_3	S	CaO
Content (%)	99.15	0.49	0.12	0.081	0.065	0.062
Component	Mn	Cr	Ni	Cu	Zn	Others
Content (%)	0.0059	0.0047	0.0038	0.0035	0.0022	0.0119

Table 2. Chemical components of pyrrhotite.

Component	SiO_2	CaO	TFe	Zn	S	Pb
Content (%)	29.41	0.18	37.76	0.94	25.94	0.18
Component	Al_2O_3	As	K_2O	Pb	Others	
Content (%)	1.85	3.34	0.20	0.18	0.02	

Table 3. Chemical components of pyrite.

Component	SiO_2	CaO	TFe	S	Ti	MgO
Content (%)	1.67	0.19	53.07	43.84	0.20	0.13
Component	Co	Al_2O_3	MgO	As	K_2O	Others
Content (%)	0.12	0.48	0.13	0.11	0.07	0.43

2.2. Methods

2.2.1. Batch Grinding Test

The specific steps and practices for batch grinding test are as follows: (1) Add grinding materials and grinding water, determine the grinding concentration, and add the prepared samples and water to the mill, respectively. (2) Grinding: Adjust the frequency converter to control the rotation speed of the ball mill to the required rotation speed for the test, set the grinding time, and start the mill grinding until the mill automatically stops. (3) Particle-size analysis of grinding products: Pour out the grinding pulp from the mill and undergo wet screening, drying, dry screening, etc. to obtain products with the particle sizes of −3.35 + 2.36 mm, −2.36 + 1.7 mm, −1.7 + 1.18 mm, −1.18 + 0.85 mm, −0.85 + 0.6 mm, −0.6 + 0.425 mm, −0.425 + 0.3 mm, −0.3 + 0.212 mm, −0.212 + 0.15 mm, −0.15 + 0.106 mm, and −0.106 + 0.075 mm, respectively. (4) Weigh and record the product of each particle size obtained through screening and calculate the yield of each particle size and the cumulative yield under screening.

During the test, the mill rotational speed was adjusted to 10 r/min to keep the grinding ball in a cascading state. Other grinding conditions are: a medium filling ratio of 35%, grinding concentration of 75%, and grinding ball diameter of 25 mm.

2.2.2. Basis and Method for Regulating the Cascading State of Grinding Medium

Based on the grinding principle proposed by Chen [5], for this experimental mill, when the rotational speed of the mill is n < 12.43 r/min, the medium in the mill is in a cascading state; when 12.43 r/min < n < 91.5 r/min, the medium in the mill is in a throwing state; and when n = 91.5 r/min, the outermost medium in the mill begins to undergo centrifugal movement.

In this test, a frequency regulator was used to adjust the rotational speed of the mill to 10 r/min to keep the grinding medium in a cascading state.

2.2.3. Characterization of Grinding Results

The grinding test results were characterized and analyzed using the grinding dynamics model, the grinding feed-particle sizes breakage rate, and the product particle size generation rate, as follows.

(1) Grinding dynamics model.

Let R_0 be the percentage of coarse particles in the ground material, and R be the percentage of feed-particle sizes in the grinding product after the grinding time t. $\mathrm{d}R/\mathrm{d}t$ represents the amount of reduction in feed-particle sizes per unit time, also known as the grinding speed. Many scholars have proven that the grinding speed is proportional to the content of the feed-particle sizes in the mill at this instant, as shown in Equation (1).

$$\mathrm{d}R/\mathrm{d}t = -\mathrm{k}R \quad (1)$$

In Equation (1), "−" indicates that the feed-particle sizes content decreases with the extension of grinding time. The k is a proportional coefficient that is mainly related to the particle size of the grinding product. Rewrite Equation (1) and integrate it, as shown in Equation (2).

$$\ln R = -\mathrm{k}t + C \quad (2)$$

In the Equation (2), C is the integral constant. When $t = 0$, $R = R_0$, and therefore $C = \ln R_0$, the basic Equation (3) of grinding dynamics is obtained by substituting the value of C into Equation (2).

$$\ln R = -\mathrm{k}t + R_0 = R_0\mathrm{e}^{-\mathrm{k}t} \quad (3)$$

Equation (3) is the most commonly used first-order grinding dynamics equation.

In this study, the grinding results were fitted according to the first-order dynamics equation, and on this basis, the grinding dynamics characteristics and differences of different mineral samples were studied.

(2) Feed-particle sizes breakage rate and product particle size generation rate.

The calculation methods for the feed-particle sizes breakage rate and the product particle size generation rate are shown in Equations (4) and (5) [27,28], respectively.

$$\text{Breakage rate}=\frac{\text{Mass of feed-particle sizes before grinding - Mass of feed-particle sizes after grinding}}{\text{Mass of feed-particle sizes before grinding}}\times 100\% \quad (4)$$

According to Equation (4), the characteristics and rules of the change of the breakage rate of the feed-particle sizes with time can be obtained.

$$\text{Generation rate}=\frac{\text{Mass of this particle size after grinding - Mass of this particle size in the feed}}{\text{Mass of this particle size in the feed}}\times 100\% \quad (5)$$

According to Equation (5), the characteristics and laws of the generation rate of different product particle sizes over time can be obtained.

(3) Characteristic particle size yield value t_{10}.

When measuring the crushing effect of a material, the particle size of the crushing product that is less than one tenth of the feed-particle sizes is often used as a characteristic particle size [29–31]. The t_{10} is also often used as an important parameter for grinding modeling in grinding process research [32,33]. The literature shows that [34–36] t_{10} is the only parameter related to the particle-size distribution of grinding products. The cumulative yield under screen corresponding to this characteristic particle size can reflect the degree of crushing of the material, which is recorded as t_{10}. t_{10} can be used to study the crushing degree and regularity of grinding products under different grinding conditions.

3. Results and Discussion

3.1. Grinding Behavior and Dynamics of Quartz during Low Grinding Speed

Based on Section 2.2.1, the grinding results of three different feed-particle sizes −3.35 + 2.36 mm, −2.36 + 1.7 mm, and −1.7 + 1.18 mm at 0.5 min, 1 min, 2 min, 4 min, and 8 min grinding time were investigated, and the particle-size distribution characteristics and grinding behavior characteristics of the products were studied.

3.1.1. Particle-Size Distribution and Grinding Behavior Characteristics of Quartz Grinding Products

(1) −3.35 + 2.36 mm feed-particle size.

The variation of the product yield of each grinding particle size with grinding time for a −3.35 + 2.36 mm feed-particle size is shown in Figure 1. Considering the significant differences in the yield of each sieve particle size in the grinding product, the grinding product is divided into +0.425 mm particle sizes and −0.425 mm particle sizes for plotting.

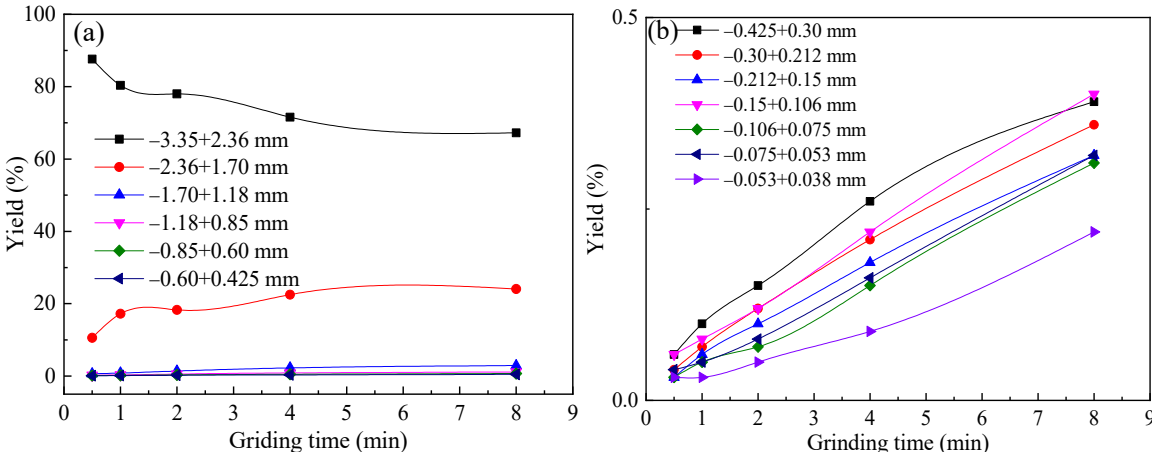

Figure 1. Diagrams of the yield varying of each particle size with grinding time for −3.35 + 2.36 mm feed quartz: (**a**) +0.425 mm each particle size and (**b**) −0.425 mm each particle size.

From Figure 1, it can be seen that the −3.35 + 2.36 mm feed-particle size is crushed in a cascading state of grinding media to produce products of various fine particle sizes. The yield of the feed-particle size itself continuously decreases with the prolongation of grinding time, while the yield of each newly generated fine particle size increases with the prolongation of the grinding time. However, Figure 1 clearly shows that during grinding for up to 8 min, the main particle sizes of the grinding products are −3.35 + 2.36 mm and −2.36 + 1.7 mm, with a total yield of over 90% for both particle sizes. The maximum yield of the second particle size (−2.36 + 1.7 mm) reached 24.08%, while the yield of the other fine particle sizes was very low, with a maximum of 2.9%. This indicates that during the 8-min grinding process, the −3.35 + 2.36 mm feed-particle size was mainly crushed to produce a second particle size (−2.36 + 1.7 mm).

As can be seen from Figure 1a, when the ordinate size range is large, the variation curve of the yield of the third particle size (−1.7 + 1.18 mm) with grinding time has tended to be flat. When the ordinate scale is further reduced, as shown in Figure 1b, the yield of each −0.425 mm particle size at 8-min does not exceed 0.5%, indicating that the generation rate of these particle sizes under grinding is very slow. It can be seen that grinding medium in a cascading state is a low-speed operation and low-energy input process. The abrasion force of the medium is relatively weak and requires repeated grinding to promote the crushing of ores.

It can also be seen from Figure 1 that, except for the production rates of −3.35 + 2.36 mm and −2.36 + 1.7 mm particle sizes, the changes in production rates of other particle sizes with grinding time exhibit linear characteristics, consistent with the characteristics of the first-order grinding dynamics model. Linear fitting was performed on the changes in the yield of newly generated fine particle products with grinding time, except for the two particle sizes of −3.35 + 2.36 mm and −2.36 + 1.7 mm. The fitting results are shown in Table 4 where $f(t)$ represents the yield of a particle size at time t and k represents the generation rate constant of the particle size.

Table 4. Fitting results of grinding dynamics for quartz grinding at −3.35 + 2.36 mm feed-particle size.

Particle Size (mm)	Intercept	k	$f(t)$	R^2
−1.7 + 1.18	0.6470	0.3069	$f(t) = 0.6470 + 0.3069 \times t$	0.9327
−1.18 + 0.85	0.2578	0.1183	$f(t) = 0.2578 + 0.1183 \times t$	0.9285
−0.85 + 0.6	0.1497	0.0722	$f(t) = 0.1497 + 0.0722 \times t$	0.9461
−0.6 + 0.425	0.0921	0.0515	$f(t) = 0.0921 + 0.0515 \times t$	0.9720
−0.425 + 0.3	0.0574	0.0435	$f(t) = 0.0574 + 0.0435 \times t$	0.9786

−0.3 + 0.212	0.0292	0.0422	$f(t) = 0.0292 + 0.0422 \times t$	0.9932
−0.212 + 0.15	0.0200	0.0381	$f(t) = 0.0200 + 0.0381 \times t$	0.9956
−0.15 + 0.106	0.0342	0.0458	$f(t) = 0.0342 + 0.0458 \times t$	0.9992
−0.106 + 0.075	0.0058	0.0375	$f(t) = 0.0058 + 0.0375 \times t$	0.9938
−0.075 + 0.053	0.0121	0.0380	$f(t) = 0.0121 + 0.0380 \times t$	0.9956
−0.053 + 0.038	0.0034	0.0265	$f(t) = 0.0034 + 0.0265 \times t$	0.9734
−0.038	0.3589	0.0957	$f(t) = 0.3589 + 0.0957 \times t$	0.9875

From Table 4, it can be seen that when the variation of the yield of each particle size with grinding time is fitted using a linear equation, the goodness of fit is greater than 0.9, indicating a high degree of linearity. In particular when the particle size generated is less than 0.6 mm, the goodness of fit is greater, reaching above 0.97. This indicates that under the experimental conditions, the yield of the newly produced fine particle size conforms to the characteristics of linear change with grinding time. In addition, after fitting and regression analysis of the data in Figure 1, t_{10} for the particle size of −3.35 + 2.36 mm at different grinding times was obtained. The result is that when the grinding time is 0.5 min, 1 min, 2 min, 4 min, and 8 min, the t_{10} is 0.52%, 1.04%, 1.33%, 2.2%, and 3.61%, respectively. It can be seen that the degree of fragmentation of quartz under the action of grinding is small, resulting in fewer fine particles.

(2) −2.36 + 1.7 mm feed-particle size.

The variation of the product yield of each grinding particle size with grinding time for a −2.36 + 1.7 mm feed-particle size is shown in Figure 2.

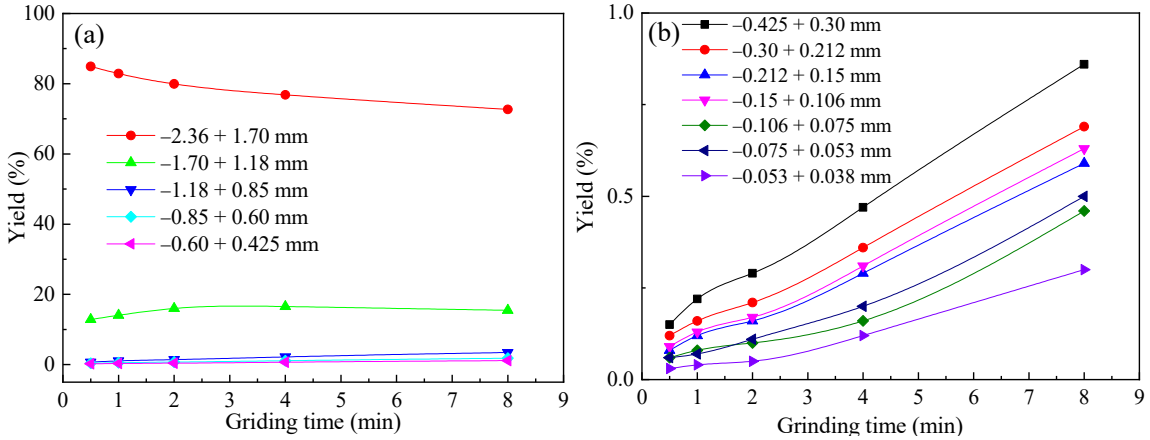

Figure 2. Diagrams of the yield varying of each particle size with grinding time for −2.36 + 1.7 mm feed quartz: (**a**) +0.425 mm each particle size and (**b**) −0.425 mm each particle size.

In general, the rule of crushing and generating each particle size of the −2.36 + 1.7 mm feed-particle size reflected in Figure 2 is basically consistent with that of the −3.35 + 2.36 mm feed-particle size. The yield of the feed-particle size itself continuously decreases with the prolongation of grinding time, while the yield of each newly generated fine particle size increases with the prolongation of grinding time. During the grinding process, the second particle size (−1.7 + 1.18 mm) particles were mainly generated from the −2.36 + 1.7 mm feed-particle size. Within 8 min, the highest yield of the second particle size was 16.53%, and the highest yield of the other particle sizes did not exceed 3.44%. From Figure 2b, it can be seen that the yield variation range of each fine particle size generated by the −2.36 + 1.7 mm feed is higher than that of the −3.35 + 2.36 mm feed, but the yield of each fine particle size at 8 min is still not more than 1%. This indicates that the grinding medium in a cascading state has a poor crushing effect on quartz.

Figure 2 also shows that, except for the yields of the two particle sizes −2.36 + 1.7 mm and −1.7 + 1.18 mm, the changes in the yields of other particle sizes with grinding time exhibit a linear characteristic, consistent with the characteristics of the first-order grinding dynamics model. Linear fitting was performed on the variation of the yield of newly generated fine particle products with grinding time, except for the two particle sizes −2.36 + 1.7 mm and −1.7 + 1.18 mm. The fitting results are shown in Table 5.

Table 5. Fitting results of grinding dynamics for quartz grinding at −2.36 + 1.7 mm feed-particle size.

Particle Size (mm)	Intercept	*k*	*f*(*t*)	R^2
−1.18 + 0.85	0.6643	0.3532	$f(t) = 0.6643 + 0.3532 \times t$	0.9920
−0.85 + 0.6	0.3316	0.1893	$f(t) = 0.3316 + 0.1893 \times t$	0.9951
−0.6 + 0.425	0.1825	0.1198	$f(t) = 0.1825 + 0.1198 \times t$	0.9987
−0.425 + 0.3	0.1097	0.0922	$f(t) = 0.1097 + 0.0922 \times t$	0.9974
−0.3 + 0.212	0.0727	0.0755	$f(t) = 0.0727 + 0.0755 \times t$	0.9958
−0.212 + 0.15	0.0388	0.0669	$f(t) = 0.0388 + 0.0669 \times t$	0.9934
−0.15 + 0.106	0.0429	0.0727	$f(t) = 0.0429 + 0.0727 \times t$	0.9927
−0.106 + 0.075	0.0079	0.0536	$f(t) = 0.0079 + 0.0536 \times t$	0.9459
−0.075 + 0.053	0.0053	0.0571	$f(t) = 0.0053 + 0.0571 \times t$	0.9648
−0.053 + 0.038	0.0059	0.0375	$f(t) = 0.0059 + 0.0375 \times t$	0.9712
−0.038	0.1964	0.1461	$f(t) = 0.1964 + 0.1461 \times t$	0.9720

As can be seen from Table 5, except for the feed-particle size itself and the second particle size closest to it, when the changes in the yield of the other 11 particle sizes with grinding time are fitted using a linear equation, the linear consistency is high. That is, under the experimental conditions, the yield of the newly produced fine particle sizes varies linearly with grinding time. The results are consistent with the grinding results of −3.35 + 2.36 mm feed listed in Table 4. In addition, a fitting and regression analysis of the data in Figure 2 can obtain the t_{10} of −2.36 + 1.7 mm quartz particles at different grinding times. The result is that when the grinding time is 0.5 min, 1 min, 2 min, 4 min, and 8 min, the t_{10} is 0.69%, 0.90%, 1.19%, 1.98%, and 4.04%, respectively. This indicates that the degree of breakage of quartz with this particle size is small under the action of grinding, and the resulting fine particle size is small.

(3) −1.7 + 1.18 mm feed-particle size.

The grinding results are shown in Figure 3.

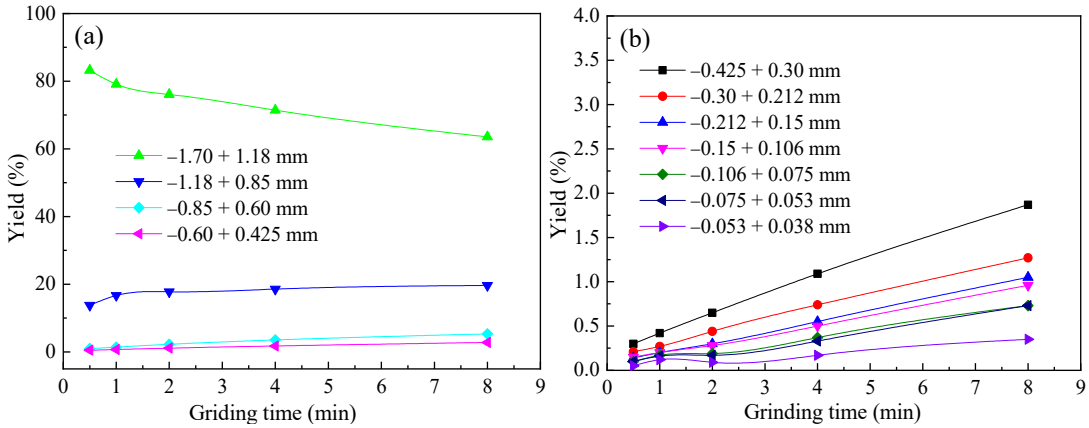

Figure 3. Diagrams of the yield varying of each particle size with grinding time for −1.7 + 1.18 mm feed quartz: (**a**) +0.425 mm each particle size and (**b**) −0.425 mm each particle size.

The crushing rule of the −1.7 + 1.18 mm feed-particle size in the grinding medium cascading state reflected in Figure 3 is basically consistent with the coarser feed-particle sizes of −3.35 + 2.36 mm and −2.36 + 1.7 mm. During the grinding process, the −1.7 + 1.18 mm feed-particle size mainly produces a second particle size (−1.18 + 0.85 mm) of particles. In different grinding times, the highest yield of the second particle size was 19.65%, and the highest yield of the other particle sizes was 5.34%. As can be seen from Figure 3b, the yield variation range of each fine particle size generated by the −1.7 + 1.18 mm feed is higher than that of the two coarser particle sizes −3.35 + 2.36 mm and −2.36 + 1.7 mm feed, but the yield of each fine particle size at 8 min does not exceed 1.87%. This indicates that although reducing the feed-particle size can promote the generation of fine particles, the total fine particle size generated is still very small.

As shown in Figures 1–3, except for the yields of −1.7 mm + 1.18 and −1.18 + 0.85 mm particle sizes, the changes in the yields of other particle sizes with grinding time exhibit linear characteristics, which also conform to the characteristics of the first-order grinding dynamics model. Linear fitting was performed on the variation of the yield of each newly generated fine particle product with grinding time, except for the two particle sizes −1.7 + 1.18 mm and −1.18 + 0.85 mm. The fitting results are shown in Table 6.

Table 6. Fitting results of grinding dynamics for quartz grinding at −1.7 + 1.18 mm feed-particle size.

Particle Size (mm)	Intercept	k	$f(t)$	R^2
−0.85 + 0.6	0.9229	0.5745	$f(t) = 0.9229 + 0.5745 \times t$	0.9756
−0.6 + 0.425	0.4392	0.3054	$f(t) = 0.4392 + 0.3054 \times t$	0.9891
−0.425 + 0.3	0.2188	0.2088	$f(t) = 0.2188 + 0.2088 \times t$	0.9980
−0.3 + 0.212	0.1447	0.1429	$f(t) = 0.1447 + 0.1429 \times t$	0.9981
−0.212 + 0.15	0.0706	0.1222	$f(t) = 0.0706 + 0.1222 \times t$	0.9991
−0.15 + 0.106	0.0817	0.1085	$f(t) = 0.0817 + 0.1085 \times t$	0.9970
−0.106 + 0.075	0.0554	0.0822	$f(t) = 0.0554 + 0.0822 \times t$	0.9896
−0.075 + 0.053	0.0404	0.0832	$f(t) = 0.0404 + 0.0832 \times t$	0.9781
−0.053 + 0.038	0.0411	0.0360	$f(t) = 0.0411 + 0.0360 \times t$	0.9296
−0.038	0.3196	0.1640	$f(t) = 0.3196 + 0.1640 \times t$	0.9922

As can be seen from Table 6, except for the feed-particle size itself and the second particle size closest to it, when the changes in the yield of other particle sizes with grinding time are fitted using a linear equation, the linear coincidence is high. In addition, fitting regression analysis was performed on the data processing in Figure 3 to obtain the t_{10} of −1.7 + 1.18 mm quartz particles at different grinding times. The result is that when the grinding time is 0.5 min, 1 min, 2 min, 4 min, and 8 min, the t_{10} is 0.88%, 1.37%, 1.66%, 2.58%, and 4.79%, which is at a lower level than the past.

According to the grinding tests of the three feed-particle sizes of quartz described above, except for the grinding process of the feed-particle size and the generation process of the second particle size closest to it, which do not conform to linear laws, the generation process of products of all other particle sizes conforms to linear laws. The reason may be that quartz has high purity, high hardness, and uniform and stable properties, resulting in slow grinding and crushing, and fewer fine particle sizes.

3.1.2. Comparative Analysis of Grinding with Different Feed-Particle Sizes

In order to further study the influence of feed-particle sizes, the grinding data of the aforementioned three feed-particle sizes −3.35 + 2.36 mm, −2.36 + 1.7 mm, and −1.7 + 1.18 mm were compared and analyzed. The breakage rates of the three feed-particle sizes of quartz calculated by Equation (4) are shown in Figure 4a. The variation of t_{10} values of grinding products of three feed-particle sizes with grinding time is shown in Figure 4b.

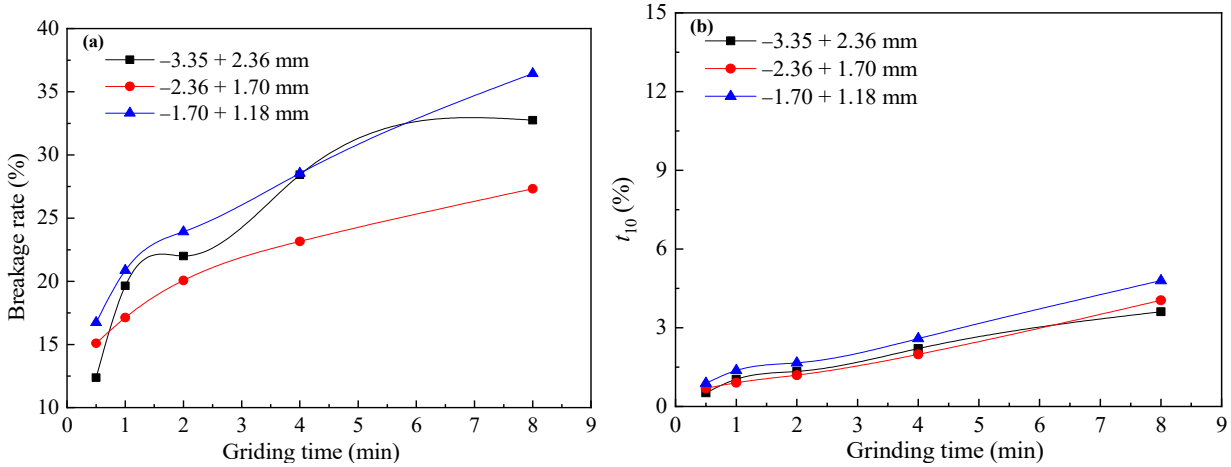

Figure 4. (**a**) The breakage rates of the three feed-particle sizes of quartz with grinding time, and (**b**) the t_{10} of the three feed-particle sizes of quartz with grinding time.

It can be seen from Figure 4 that the breakage rates of the three feed-particle sizes of quartz increase with the increase of grinding time, but the increase rate from 2 to 8 min is smaller than that from 0.5 to 2 min. This indicates that with the increase of grinding time, the increase rate of quartz breakage rate slows down and the curve slope decreases. The reason may be related to the surface defects of quartz particles; that is, at the beginning of grinding, due to the irregular shape of broken particles, there are many surface defects. After grinding for a period of time, the particle surface defects basically disappear, so the grinding speed decreases and enters a stable grinding state. At the same time, when the particles are small enough, there is a condensation phenomenon in the fine particle group, and grinding no longer has an effect. For the three feeding-particle sizes of quartz, the breakage rate of the −1.70 + 1.18 mm feed-particle size is the highest, and the increase rate is faster. This indicates that under the same quality, the specific surface area of the smallest feed-particle size is the largest, and the effective contact area of quartz particles with the grinding medium is the largest, so its breakage rate changes faster with grinding time. The breakage rate of the −3.35 + 2.36 mm feed-particle size is in the middle, while the breakage rate and its increase rate of the −2.36 + 1.7 mm feed-particle size are the smallest. It can be seen that when the medium in the mill is in a cascading state, the breakage rate and increase rate of quartz are not completely positively correlated with the size of the feed-particle size, and the reason for this phenomenon needs further research.

However, it is worth noting that during the entire grinding process, the variation trend and absolute value of t_{10} for the three feed-particle sizes are very close, and the absolute value is not significant. After 8 min of grinding, the maximum value is less than 6%.

3.2. Grinding Behavior and Dynamics of Pyrrhotite during Low Grinding Speed

3.2.1. Particle-Size Distribution and Grinding Behavior Characteristics of Pyrrhotite Grinding Products

(1) −3.35 + 2.36 mm feed-particle size.

The grinding results are shown in Figure 5.

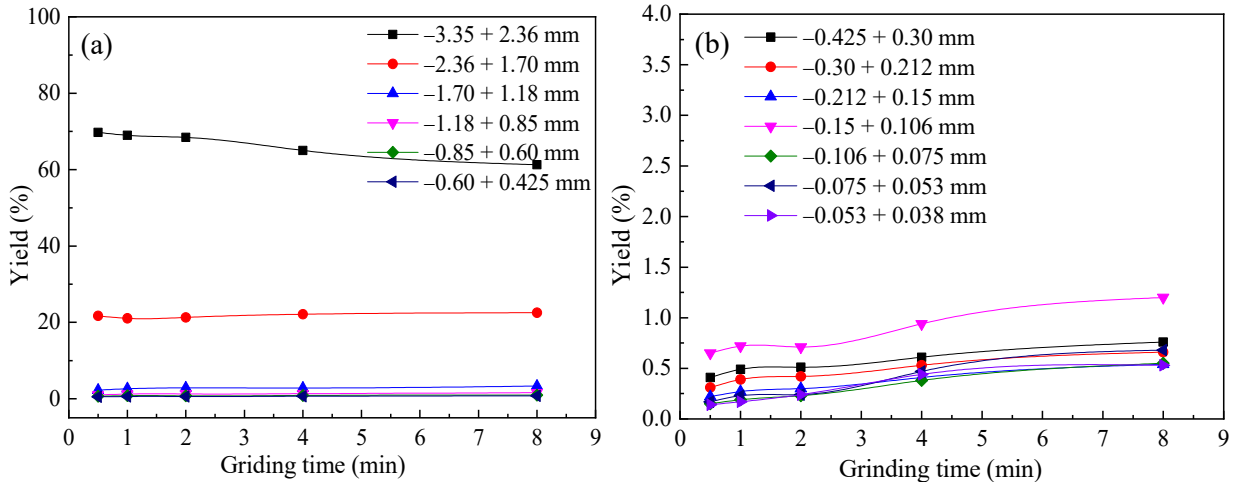

Figure 5. Diagrams of the yield varying of each particle size with grinding time for −3.35 + 2.36 mm feed pyrrhotite: (**a**) +0.425 mm each particle size and (**b**) −0.425 mm each particle size.

It can be seen from Figure 5 that, like quartz grinding, the yield of the −3.35 + 2.36 mm feed-particle size continuously decreases with the prolongation of grinding time, while the yield of each newly generated fine particle size increases with the prolongation of grinding time, in line with conventional grinding rules. During grinding for up to 8 min, the main particle sizes of the grinding product are −3.35 + 2.36 mm and −2.36 + 1.7 mm, while the yield of other fine particle sizes is very low, with a maximum of no more than 3.32%. This also indicates that during the grinding process, pyrrhotite particles with a particle size of −3.35 + 2.36 mm mainly generate particles with a second particle size (−2.36 + 1.7 mm), and the maximum yield of the second particle size is 22.52% at different grinding times.

As can be seen from Figure 5a, when the ordinate range is large, the variation curve of the yield of the third particle size (−1.7 + 1.18 mm) with grinding time has tended to be flat. As shown in Figure 5b, the yield of each particle size of −0.425 mm at 8 min does not exceed 0.76%, indicating that the generation rate of these particle sizes under grinding is extremely slow. Therefore, the grinding of pyrrhotite once again proves that the cascading state, as a low-speed operation and low-energy input consumption process, requires repeated grinding to promote the occurrence of crushing behavior.

Similarly, according to the variation characteristics of the yield of each particle size of the product with grinding time in Figure 5, the results shown in Table 7 are obtained by fitting a first-order grinding dynamics model for each fine particle size below −0.6 mm.

Table 7. Fitting results of grinding dynamics for pyrrhotite grinding at −3.35 + 2.36 mm feed-particle size.

Particle Size (mm)	Intercept	*k*	*f*(*t*)	R^2
−0.6 + 0.425	0.5199	0.0330	$f(t) = 0.5199 + 0.0330 \times t$	0.9520
−0.425 + 0.3	0.4207	0.0445	$f(t) = 0.0574 + 0.0435 \times t$	0.9685
−0.3 + 0.212	0.3260	0.0448	$f(t) = 0.0292 + 0.0422 \times t$	0.9552
−0.212 + 0.15	0.2192	0.0416	$f(t) = 0.0200 + 0.0381 \times t$	0.9750
−0.15 + 0.106	0.6154	0.0737	$f(t) = 0.0342 + 0.0458 \times t$	0.9800
−0.106 + 0.075	0.1333	0.0544	$f(t) = 0.0058 + 0.0375 \times t$	0.9853
−0.075 + 0.053	0.1442	0.0690	$f(t) = 0.0121 + 0.0380 \times t$	0.9642
−0.053 + 0.038	0.1361	0.0550	$f(t) = 0.0034 + 0.0265 \times t$	0.9600
−0.038	1.8296	0.3569	$f(t) = 0.3589 + 0.0957 \times t$	0.9458

From Table 7, it can be seen that when the variation of the yield of each particle size of −0.6 mm in the grinding product of pyrrhotite feed with grinding time is fitted according to the first-order grinding dynamics linear equation, the linear coincidence degree is high, consistent with the generation law of quartz-grinding products. In addition, processing and fitting regression analysis of the data in Figure 5 can obtain the t_{10} of the −3.35 + 2.36 mm particle size pyrrhotite feed at different grinding times. The result is that when the grinding time is 0.5 min, 1 min, 2 min, 4 min, and 8 min, the t_{10} is 4.26%, 4.65%, 4.69%, 7.07%, and 9.31%, respectively. This result is higher than that of quartz, which should be related to the relatively low purity of pyrrhotite and the magnetic nature of pyrrhotite, which needs further research.

(2) −2.36 + 1.7 mm feed-particle size.

The grinding results are shown in Figure 6.

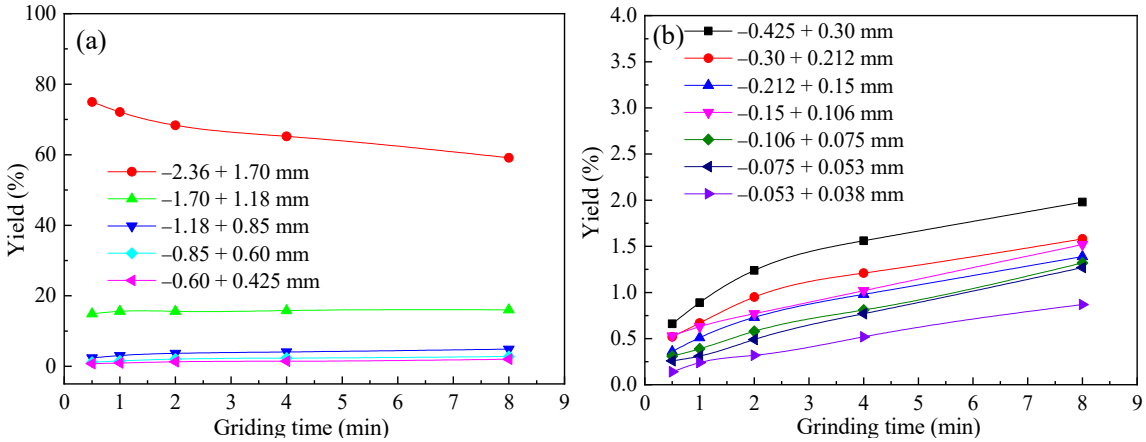

Figure 6. Diagrams of the yield varying of each particle size with grinding time for −2.36 + 1.7 mm feed pyrrhotite: (**a**) +0.425 mm each particle size and (**b**) −0.425 mm each particle size.

In general, the rule of the generation of each particle size of the −2.36 + 1.7 mm feed-particle size under grinding as reflected in Figure 6 is basically consistent with the rule of the −3.35 + 2.36 mm feed-particle size. During the grinding process, the yield of the second particle size (−1.7 + 1.18 mm) changed relatively gently, with a minimum yield of 14.87% and a maximum yield of 16.01%. The yield of the other particle sizes did not exceed 4.86%. From Figure 6b, it can be seen that the yield variation range of each fine particle size generated by the −2.36 + 1.7 mm feed is higher than that of the −3.35 + 2.36 mm feed, but the yield of each fine particle size at 8 min does not exceed 1.98%.

Figure 6 also shows that the yield of each particle size of −0.6 mm in the grinding product exhibits a linear characteristic as a function of grinding time, consistent with the characteristics of a first-order grinding dynamics model. Linear fitting was performed on the yield of each newly generated fine particle size product of −0.6 mm as a function of grinding time, and the fitting results are shown in Table 8.

Table 8. Fitting results of grinding dynamics for pyrrhotite grinding at −2.36 + 1.7 mm feed-particle size.

Particle Size (mm)	Intercept	*k*	*f*(*t*)	R^2
−0.6 + 0.425	0.7952	0.1599	$f(t) = 0.7952 + 0.1599 \times t$	0.9618
−0.425 + 0.3	0.7531	0.1652	$f(t) = 0.7531 + 0.1652 \times t$	0.9564
−0.3 + 0.212	0.5671	0.1351	$f(t) = 0.5671 + 0.1351 \times t$	0.9524
−0.212 + 0.15	0.3871	0.1313	$f(t) = 0.3871 + 0.1313 \times t$	0.9558
−0.15 + 0.106	0.4925	0.1295	$f(t) = 0.4925 + 0.1295 \times t$	0.9972
−0.106 + 0.075	0.2710	0.1323	$f(t) = 0.2710 + 0.1323 \times t$	0.9950

−0.075 + 0.053	0.1990	0.1361	$f(t) = 0.1990 + 0.1361 \times t$	0.9968
−0.053 + 0.038	0.1254	0.0944	$f(t) = 0.1254 + 0.0944 \times t$	0.9924
−0.038	3.0541	0.2924	$f(t) = 3.0541 + 0.2924 \times t$	0.9416

From Table 8, it can be seen that among the grinding products with a feed size of −2.36 + 1.7 mm, the variation of the yield of the −0.6 mm particle size with grinding time conforms to a linear variation characteristic. In addition, after processing the data in Figure 6 and performing a regression analysis, the t_{10} values of −2.36 + 1.7 mm particle size pyrrhotite at different grinding times were obtained. The result is that when the grinding time is 0.5 min, 1 min, 2 min, 4 min, and 8 min, the t_{10} is 4.84%, 5.46%, 7.15%, 8.74%, and 12.01%, respectively. This result is higher than the feed-particle size of −3.35 + 2.36 mm pyrrhotite, and also higher than the yield of quartz at the same feed-particle size.

(3) −1.7 + 1.18 mm feed-particle size.

The grinding results are shown in Figure 7.

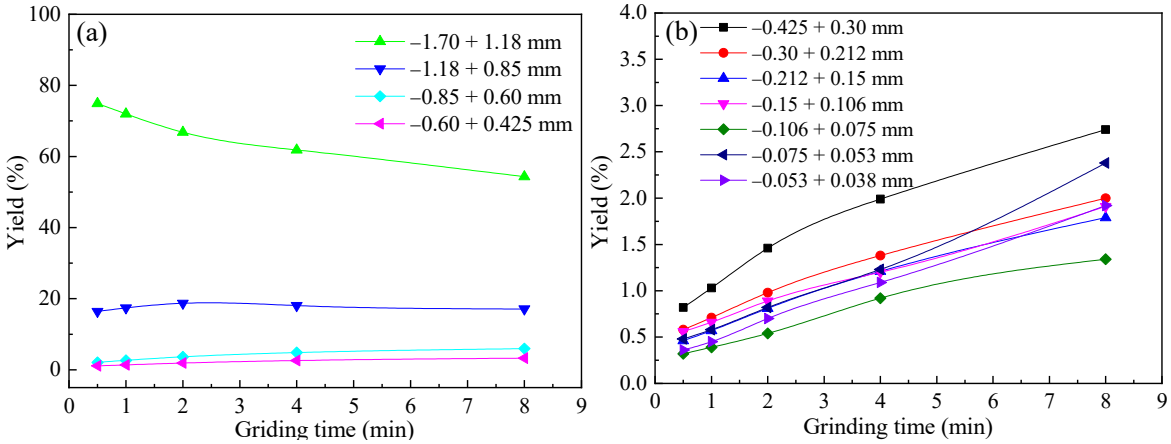

Figure 7. Diagrams of the yield varying of each particle size with grinding time for −1.7 + 1.18 mm feed pyrrhotite: (**a**) +0.425 mm each particle size and (**b**) −0.425 mm each particle size.

On the whole, the rule of generation of each particle level in the cascading state for the −1.7 + 1.18 mm feed-particle size reflected in Figure 7 is basically consistent with that for the −3.35 + 2.36 mm and −2.36 + 1.7 mm feed-particle sizes. During the grinding process, the maximum yield of the second particle size (−1.18 + 0.85 mm) was 18.73%, and the maximum yield of the other particle sizes was 5.96%. As can be seen from Figure 7b, the yield variation range of each fine particle size generated by the −1.7 + 1.18 mm feed is higher than that of the −3.35 + 2.36 mm and −2.36 + 1.7 mm feed, but the yield of each fine particle size at 8 min does not exceed 2.74%, which is still at a relatively low yield.

Figure 7 also shows that the yield of each particle size of −0.6 mm in the grinding product exhibits a linear characteristic as a function of grinding time. Linear fitting was performed on the yield of each newly generated fine particle size product of −0.6 mm as a function of grinding time, and the fitting results are shown in Table 9.

Table 9. Fitting results of grinding dynamics for pyrrhotite grinding at −1.7 + 1.18 mm feed-particle size.

Particle Size (mm)	Intercept	*k*	*f(t)*	R^2
−0.6 + 0.425	1.1808	0.2843	$f(t) = 1.1808 + 0.2843 \times t$	0.9591
−0.425 + 0.3	0.8317	0.2504	$f(t) = 0.8317 + 0.2504 \times t$	0.9605
−0.3 + 0.212	0.5496	0.1872	$f(t) = 0.5496 + 0.1872 \times t$	0.9831
−0.212 + 0.15	0.4200	0.1768	$f(t) = 0.4200 + 0.1768 \times t$	0.9850
−0.15 + 0.106	0.4925	0.1779	$f(t) = 0.4925 + 0.1779 \times t$	0.9973

−0.106 + 0.075	0.2729	0.1384	$f(t) = 0.2729 + 0.1384 \times t$	0.9790
−0.075 + 0.053	0.3143	0.2532	$f(t) = 0.3143 + 0.2532 \times t$	0.9944
−0.053 + 0.038	0.2592	0.2080	$f(t) = 0.2592 + 0.2080 \times t$	0.9992
−0.038	1.7196	0.4453	$f(t) = 1.7196 + 0.4453 \times t$	0.9967

From Table 9, it can be seen that when the variation of the yield of each particle size of −0.6 mm in the grinding product with a feed-particle size of −1.7 + 1.18 mm as a function of grinding time is fitted by a linear equation, the linear coincidence is high. After processing the data in Figure 7, fitting regression analysis was performed to obtain t_{10} at different grinding times. The result is that when the grinding time is 0.5 min, 1 min, 2 min, 4 min, and 8 min, the t_{10} is 3.82%, 4.46%, 5.93%, 8.33%, and 13.01%, respectively. This size comparison relationship is similar to its two coarser particle sizes. Therefore, this once again proves that the difference in material properties between pyrrhotite samples and quartz samples affects the grinding effect.

3.2.2. Comparative Analysis of Grinding with Different Feed-Particle Sizes

Comparative analysis was conducted on the grinding data of pyrrhotite with three feed-particle sizes of −3.35 + 2.36 mm, −2.36 + 1.7 mm, and −1.7 + 1.18 mm. The breakage rates of the three feed-particle sizes of pyrrhotite calculated by Equation (4) are shown in Figure 8a. The variation of t_{10} values of the three feed-particle sizes with grinding time is shown in Figure 8b.

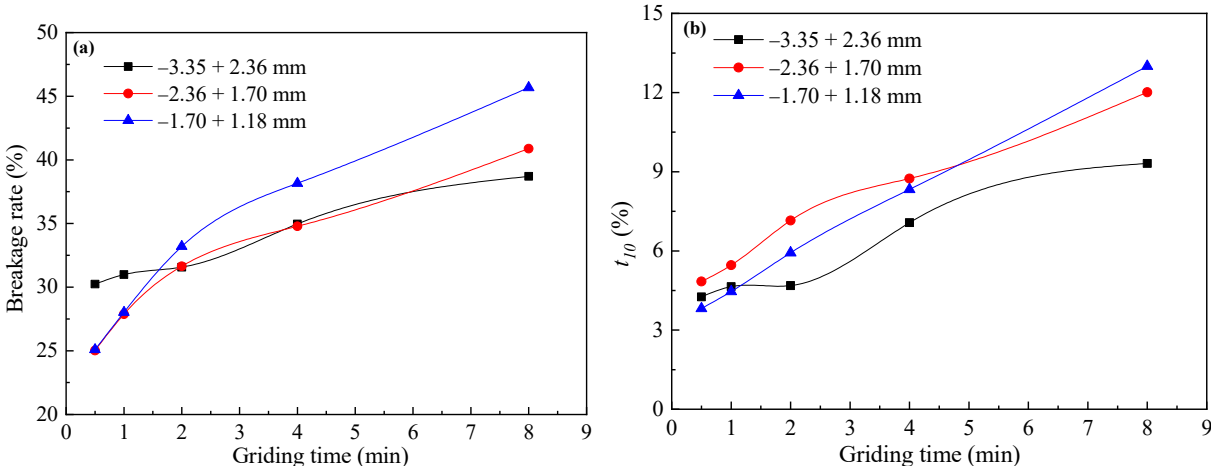

Figure 8. (**a**) The breakage rates of the three feed-particle sizes of pyrrhotite with grinding time and (**b**) the t_{10} of the three feed-particle sizes of pyrrhotite with grinding time.

From Figure 8, it can be seen that the breakage rates of the three feed-particle sizes of pyrrhotite increase with the increase of grinding time, but the increase rate of the breakage rates of −2.36 + 1.7 mm and −1.7 + 1.18 mm particle sizes gradually decreases. Moreover, the increase rate of breakage rate from 2 to 8 min is smaller than that from 0.5 to 2 min. This indicates that with the increase of grinding time, the increase rate of pyrrhotite breakage rate slows down and the curve slope decreases, which is basically consistent with the grinding results of quartz. For the three feed-particle sizes of pyrrhotite, the smallest particle size (−1.70 + 1.18 mm) has the highest breakage rate. This indicates that under the same quality, the specific surface area of the smallest particle size is the largest, and the effective contact area of pyrrhotite particles with the grinding medium is the largest, so its breakage rate changes faster with grinding time. The breakage rate of the feed with a particle size of −3.35 + 2.36 mm and a particle size of −2.36 + 1.7 mm is basically the same after 2 min of grinding time. This also proves once again that when the medium in the mill is in a cascading state, the breakage rate of pyrrhotite and its increase rate are

not completely positively correlated with the feed-particle size. As can be seen from Figure 8b, during the entire grinding and crushing process, the highest t_{10} value of the three feed-particle sizes is 13.01%, and the lowest is 3.82%, which are significantly higher than the t_{10} value of the corresponding particle size of quartz. Furthermore, the t_{10} value of the −3.35 + 2.36 mm feed-particle size is the lowest, while the t_{10} value of the grinding products of the other two feed-particle sizes is close.

3.3. Grinding Behavior and Dynamics of Pyrite during Low Grinding Speed

3.3.1. Particle-Size Distribution and Grinding Behavior Characteristics of Pyrite Grinding Products

(1) −3.35 + 2.36 mm feed-particle size.

The grinding results are shown in Figure 9.

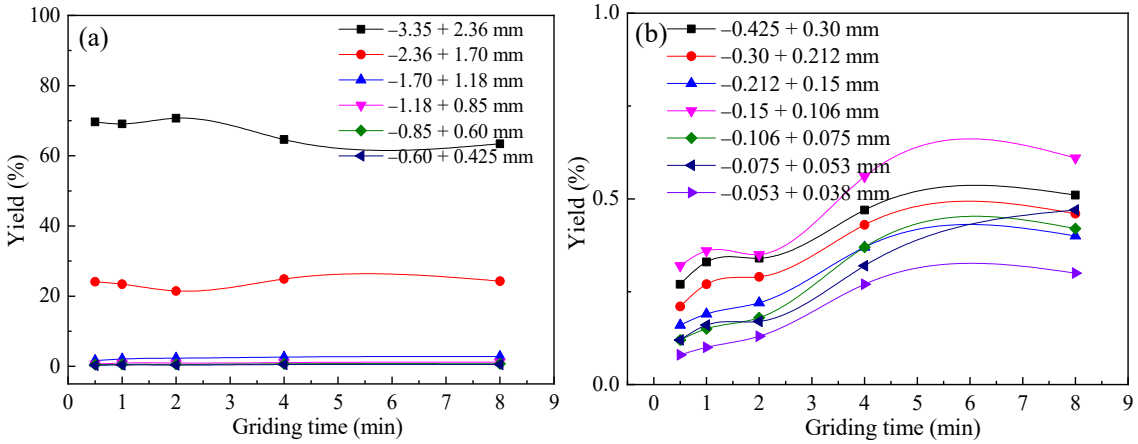

Figure 9. Diagrams of the yield varying of each particle size with grinding time for −3.35 + 2.36 mm feed pyrite, (**a**) +0.425 mm each particle size and (**b**) −0.425 mm each particle size.

From Figure 9, it can be seen that pyrite with a feed-particle size of −3.35 + 2.36 mm is broken into fine-particle-size products in a cascading state of grinding media. The yield of the feed-particle size itself continuously decreases with the extension of grinding time, and the yield of each newly generated fine-particle-size product increases with the extension of grinding time, consistent with conventional grinding rules. Similarly, during the grinding process lasting for 8 min, the main particle sizes of the grinding products are −3.35 + 2.36 mm and −2.36 + 1.7 mm. The maximum yield of the second particle size (−2.36 + 1.7 mm) was 24.89%, while the yield of the other fine particle sizes was very low, with a maximum of 2.8%. The two characteristic data of pyrite (the highest yield of the second particle size and the highest yield of each fine particle size in the product) are similar to the grinding results of quartz and pyrrhotite. Specifically, pyrite is 24.89% and 2.8%, quartz is 24.08% and 2.9%, and pyrrhotite is 22.52% and 3.32%. This indicates that under the same feed-particle size, the three minerals mainly produce products with a particle size of −2.36 + 1.7 mm under grinding action, and the highest yield is similar. This indicates that the yield of a certain particle size tends to a constant value with the increase of grinding time in the cascading state. As can be seen from Figure 9a, when the ordinate range is large, the variation curve of the yield of the third particle size (−1.7 + 1.18 mm) with grinding time has tended to be flat. When further zooming in on the ordinate, as shown in Figure 9b, the yield of each particle size of −0.425 mm did not exceed 0.51% at 8 min, indicating that the generation rate of these particle sizes was very slow.

(2) −2.36 + 1.7 mm feed-particle size.

The grinding results are shown in Figure 10.

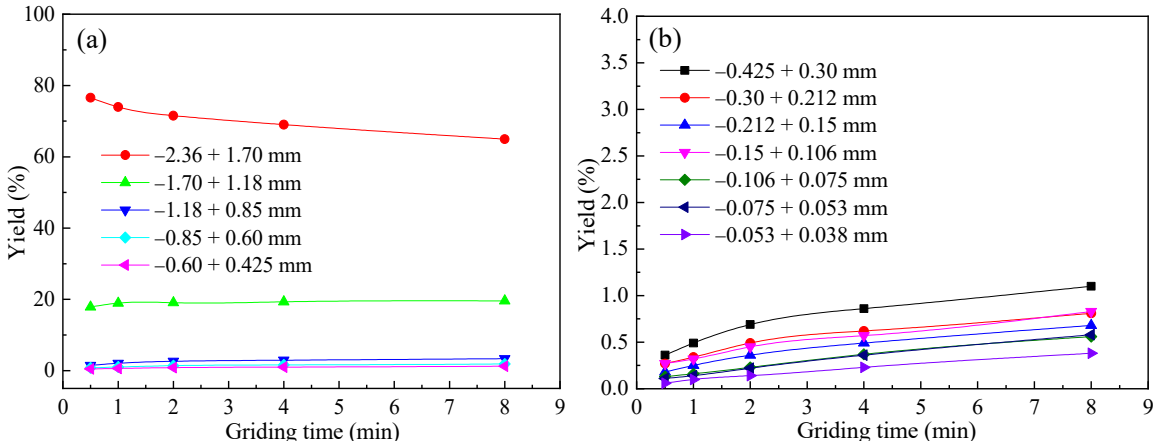

Figure 10. Diagrams of the yield varying of each particle size with grinding time for −2.36 + 1.7 mm feed pyrite: (**a**) +0.425 mm each particle size and (**b**) −0.425 mm each particle size.

As shown in Figure 10, the feed-particle size of pyrite is −2.36 + 1.7 mm, and the rule of each particle size generated by grinding is basically consistent with the feed-particle size of −3.35 + 2.36 mm. In different grinding times, the highest yield of the second particle size (−1.7 + 1.18 mm) was 19.57%, while the highest yield of the other particle sizes did not exceed 3.35%. From Figure 10b, it can be seen that the yield variation range of each fine particle size generated by the −2.36 + 1.7 mm feed is higher than that of the −3.35 + 2.36 mm feed. However, the yield of each fine particle size at 8 min is still not more than 1.10%, indicating that there are still very few small particles generated under the action of grinding.

Figure 10 also shows that the yield of each particle size of −0.425 mm in the grinding product exhibits a linear characteristic as a function of grinding time, consistent with the characteristics of a first-order grinding dynamics model. Linear fitting was performed on the yield of each newly generated fine particle product of −0.425 mm as a function of grinding time, and the fitting results are shown in Table 10.

Table 10. Fitting results of grinding dynamics for pyrite grinding at −2.36 + 1.7 mm feed-particle size.

Particle Size (mm)	Intercept	k	$f(t)$	R^2
−0.425 + 0.3	0.4101	0.0986	$f(t) = 0.4101 + 0.0986 \times t$	0.9532
−0.3 + 0.212	0.2917	0.0691	$f(t) = 0.2917 + 0.0691 \times t$	0.9617
−0.212 + 0.15	0.1933	0.0641	$f(t) = 0.1933 + 0.0641 \times t$	0.9504
−0.15 + 0.106	0.2621	0.0729	$f(t) = 0.2621 + 0.0729 \times t$	0.9780
−0.106 + 0.075	0.1108	0.0578	$f(t) = 0.1108 + 0.0578 \times t$	0.9879
−0.075 + 0.053	0.0867	0.0630	$f(t) = 0.0867 + 0.0630 \times t$	0.9930
−0.053 + 0.038	0.0529	0.0416	$f(t) = 0.0529 + 0.0416 \times t$	0.9922
−0.038	1.2521	0.3516	$f(t) = 1.2521 + 0.3516 \times t$	0.9993

From Table 10, it can be seen that the variation of the yield of −0.425 mm particle sizes in the grinding product of pyrite with a feed-particle size of −2.36 + 1.7 mm with grinding time conforms to a linear variation feature. In addition, fitting and regression analysis of the data in Figure 10 can obtain the t_{10} of pyrite with a particle size of −2.36 + 1.7 mm at different grinding times. The result is that when the grinding time is 0.5 min, 1 min, 2 min, 4 min, and 8 min, the t_{10} is 2.52%, 2.93%, 3.74%, 5.06%, and 7.55%, respectively.

(3) −1.7 + 1.18 mm feed-particle size.

The grinding results are shown in Figure 11.

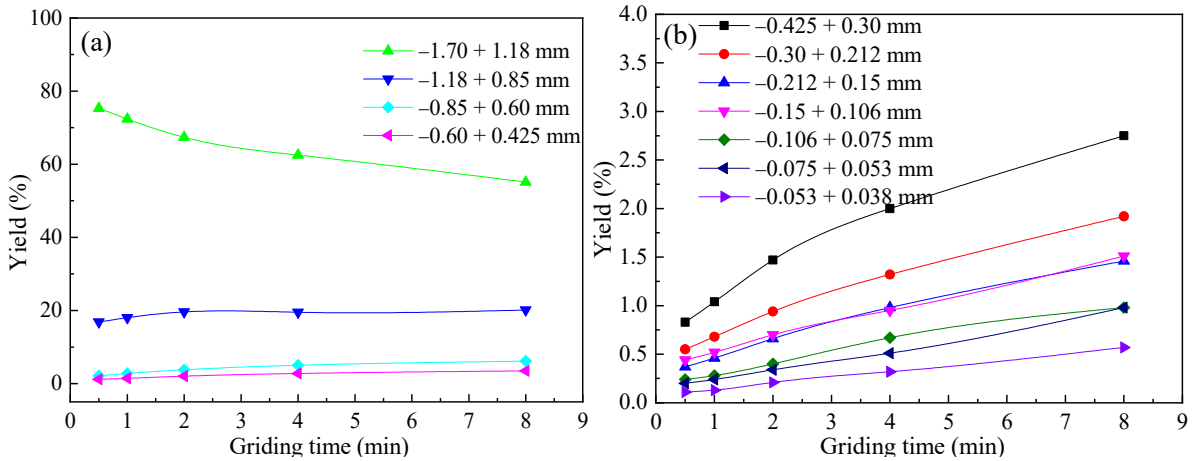

Figure 11. Diagram of the yield varying of each particle size with grinding time for −1.7 + 1.18 mm feed pyrite: (**a**) +0.425 mm each particle size and (**b**) −0.425 mm each particle size.

On the whole, the rule of grinding and producing each particle size of −1.7 + 1.18 mm feed-particle size as reflected in Figure 11 is basically consistent with that of −3.35 + 2.36 mm and −2.36 + 1.7 mm feed-particle sizes. In different grinding times, the highest yield of the second particle size (−1.18 + 0.85 mm) was 20.15%, and the highest yield of the other particle sizes was 6.15%. As can be seen from Figure 11b, the yield variation range of each fine particle size generated by the −1.7 + 1.18 mm feed is higher than that of the −3.35 + 2.36 mm and −2.36 + 1.7 mm feeds, but the yield of each fine particle size at 8 min does not exceed 2.75%. Figure 11 also shows that the yield of each particle size of −0.425 mm in the grinding product exhibits a linear characteristic as a function of grinding time. The yield of each newly generated fine particle size of −0.425 mm is linearly fitted as a function of grinding time. The fitting results are shown in Table 11.

Table 11. Fitting results of grinding dynamics for pyrite grinding at −2.36 + 1.7 mm feed-particle size.

Particle Size (mm)	Intercept	*k*	*f*(*t*)	R^2
−0.425 + 0.3	0.8417	0.2504	$f(t) = 0.8417 + 0.2504 \times t$	0.9605
−0.3 + 0.212	0.5233	0.1802	$f(t) = 0.5233 + 0.1802 \times t$	0.9831
−0.212 + 0.15	0.3375	0.1447	$f(t) = 0.3375 + 0.1447 \times t$	0.9857
−0.15 + 0.106	0.3867	0.1411	$f(t) = 0.3867 + 0.1411 \times t$	0.9976
−0.106 + 0.075	0.2013	0.1009	$f(t) = 0.2013 + 0.1009 \times t$	0.9803
−0.075 + 0.053	0.1319	0.1041	$f(t) = 0.1319 + 0.1041 \times t$	0.9948
−0.053 + 0.038	0.0771	0.0616	$f(t) = 0.0771 + 0.0616 \times t$	0.9982
−0.038	1.5963	0.4193	$f(t) = 1.5963 + 0.4193 \times t$	0.9935

As can be seen from Table 11, when the variation of the yield of each particle size of −0.425 mm in the grinding product with grinding time is fitted using a linear equation, the goodness of fit is large, indicating a high degree of linear coincidence. In addition, fitting and regression analysis of the data in Figure 11 can obtain the t_{10} of −1.7 + 1.18 mm particle size pyrite at different grinding times. The result is that when the grinding time is 0.5 min, 1 min, 2 min, 4 min, and 8 min, the t_{10} is 2.97%, 3.45%, 4.50%, 6.30%, and 9.42%, respectively. Compared to the aforementioned coarse-particle-feeding results, as the feed-particle size decreases, the t_{10} value increases. This rule is consistent with quartz and pyrrhotite.

3.3.2. Comparative Analysis of Grinding with Different Feed-Particle Sizes

Comparative analysis was conducted on the grinding data of pyrite with feed-particle sizes of −3.35 + 2.36 mm, −2.36 + 1.7 mm, and −1.7 + 1.18 mm, respectively, to obtain Figure 12a,b.

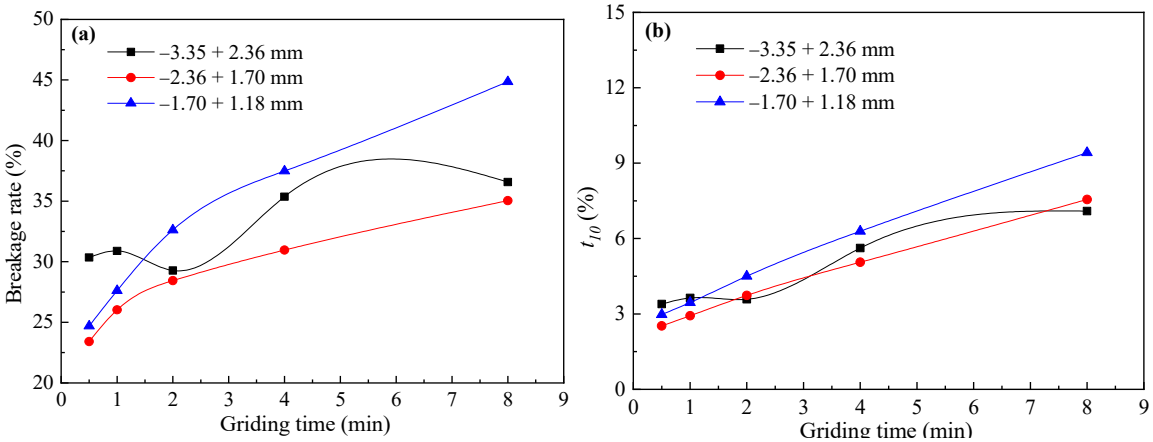

Figure 12. (**a**) The breakage rates of the three feed-particle sizes of pyrite with grinding time and (**b**) the t_{10} of the three feed-particle sizes of pyrite with grinding time.

It can be seen from Figure 12a that, like quartz and pyrrhotite, the breakage rates of the three feed-particle sizes of pyrite increase with the increase of grinding time, and the increase rate of the breakage rates of the −2.36 + 1.7 mm and −1.7 + 1.18 mm feed-particle sizes gradually decreases. This indicates that with the increase of grinding time, the increase rate of pyrite breakage rate slows down and the curve slope decreases. Among the three feed-particle sizes, the smallest particle size (−1.70 + 1.18 mm) has the highest breakage rate and a faster increase rate. The breakage rate of pyrite with a feed size of −3.35 + 2.36 mm fluctuates with the increase of grinding time, showing an overall upward trend. Therefore, when the medium in the mill is in a cascading state, the pyrite breakage rate and its increase rate are not completely positively correlated with the feed-particle size.

As can be seen from Figure 12b, the t_{10} values of the three feed-particle sizes of pyrite are relatively close during the entire grinding and crushing process. Compared with the t_{10} variation diagram of quartz and the t_{10} variation diagram of pyrrhotite, it can be seen that the t_{10} values of pyrite are significantly higher than the t_{10} values of quartz, but lower than the t_{10} values of pyrrhotite. The grinding product t_{10} value of the −1.7 + 1.18 mm feed-particle size is the highest, showing a linear increase trend with time.

3.4. Comparative Study on Grinding Characteristics of Three Minerals

In order to further study the impact of mineral sample properties on grinding characteristics, this section summarizes the grinding test results of three kinds of mineral samples, namely quartz, pyrrhotite, and pyrite, for comparative analysis and research. Figure 13 is a summary of the breakage rates for three feed-particle sizes of three kinds of minerals.

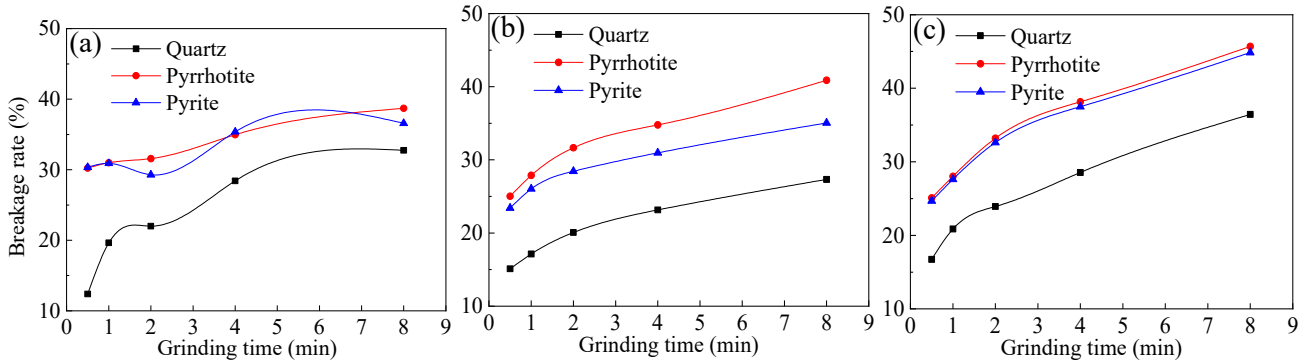

Figure 13. Comparative diagrams of the relationship between the breakage rate and grinding time for three kinds of minerals: (**a**) −3.35 + 2.36 mm feed, (**b**) −2.36 + 1.7 mm feed, and (**c**) −1.7 + 1.18 mm feed.

As can be seen from Figure 13, the breakage rates of the three minerals continue to increase with the extension of grinding time. After 2 min of grinding time, the slope of the curve decreases and the increase rate of breakage rate begins to slow down. In addition, the breakage rate of quartz is significantly lower than that of pyrrhotite and pyrite under the three feed-particle sizes. When the feed-particle size is −3.35 + 2.36 mm and −1.7 + 1.18 mm, the breakage rate of pyrrhotite is close to that of pyrite, with pyrrhotite slightly higher. To sum up, the relationship between the breakage rates of the three minerals under different feed-particle sizes is: pyrrhotite > pyrite > quartz, which means that pyrrhotite is most likely to be ground and broken.

Combining Figures 4, 8, and 12, it can be seen that the feed-particle size affects the change rule of the mineral-breakage rate. Of the three feed-particle sizes of quartz, pyrrhotite, and pyrite, the intermediate feed-particle size (−2.36 + 1.7 mm) has the lowest breakage rate. The minimum feed-particle size (−1.70 + 1.18 mm) has the highest breakage rate and the fastest increase rate. The breakage rate of the maximum feed-particle size (−3.35 + 2.36 mm) is between the other two feed-particle sizes. Therefore, when the medium in the mill is in a cascading state, the breakage rates and their increase rates of the three minerals are not completely positively correlated with the feed-particle size.

The generation rates k of the products of various particle sizes after the grinding of quartz, pyrrhotite, and pyrite are summarized to obtain Figure 14.

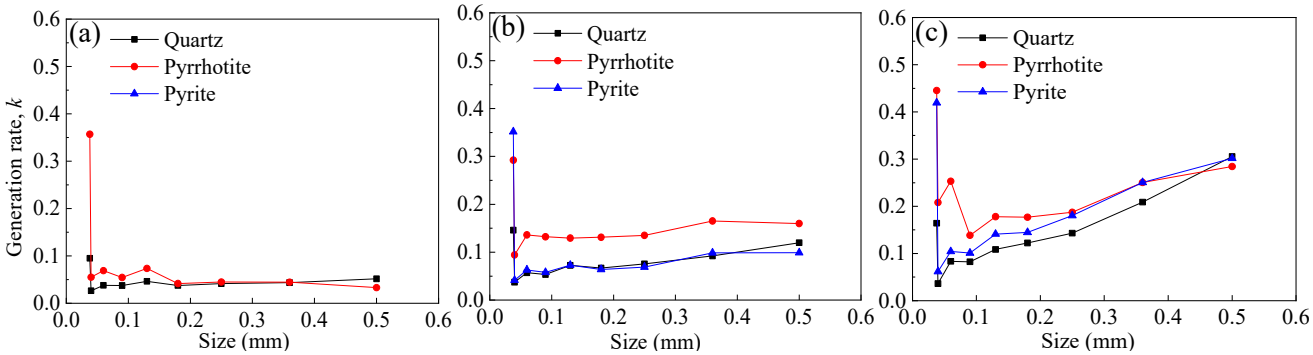

Figure 14. Generation rate comparison diagrams of each size products for three kinds of minerals after grinding: (**a**) −3.35 + 2.36 mm feed, (**b**) −2.36 + 1.7 mm feed, and (**c**) −1.7 + 1.18 mm feed.

As can be seen from Figure 14, the generation rate of each product particle size after grinding of quartz, pyrrhotite, and pyrite is relatively small. The generation rate of all particle sizes decreases as the particle size of the product decreases, except that the generation rate of the minimum particle size −0.038 mm is relatively large. This means that during the grinding process, the main task is to generate the second coarse particle

size and the fine particle size below −0.038 mm. When the feed-particle size is −3.35 + 2.36 mm, the generation rate of coarse particle size products of quartz and pyrrhotite is similar, but the generation rate of fine particle size products of quartz is lower than that of pyrrhotite. When the feed-particle size is −2.36 + 1.7 mm, the generation rates of quartz and pyrite particle sizes are similar, and significantly lower than pyrrhotite. When the feed-particle size is −1.7 + 1.18 mm, the order of the generation rates of the fine particle size products of the three minerals is: pyrrhotite > pyrite > quartz.

In summary, under the action of grinding, the generation rate of all product particle sizes is relatively low, and their size is positively correlated with the size of the product particle size, while negatively correlated with the size of the feed-particle size. The order of generation rates of grinding products for different feed-particle sizes is: −1.70 + 1.18 mm > −2.36 + 1.7 mm > −3.35 + 2.36 mm. That is, the coarser the particle size of the feed, the longer it takes for it to break and generate a specified particle size. In addition, the size of the grinding product-generation rate is negatively correlated with the mineral Mohs hardness. The greater the mineral hardness, the smaller the generation rate of grinding products.

Based on the grinding yield data of quartz, pyrrhotite, and pyrite, the relative particle size of the feed-particle size is used as the abscissa. Relative particle size, that is, the nominal particle size of the feed-particle size is the denominator and the nominal particle size of each product particle size is the numerator. Comparative studies were conducted on the yield of each product particle size and the cumulative yield under sieve after grinding with different feed-particle sizes and the results are shown in Figure 15.

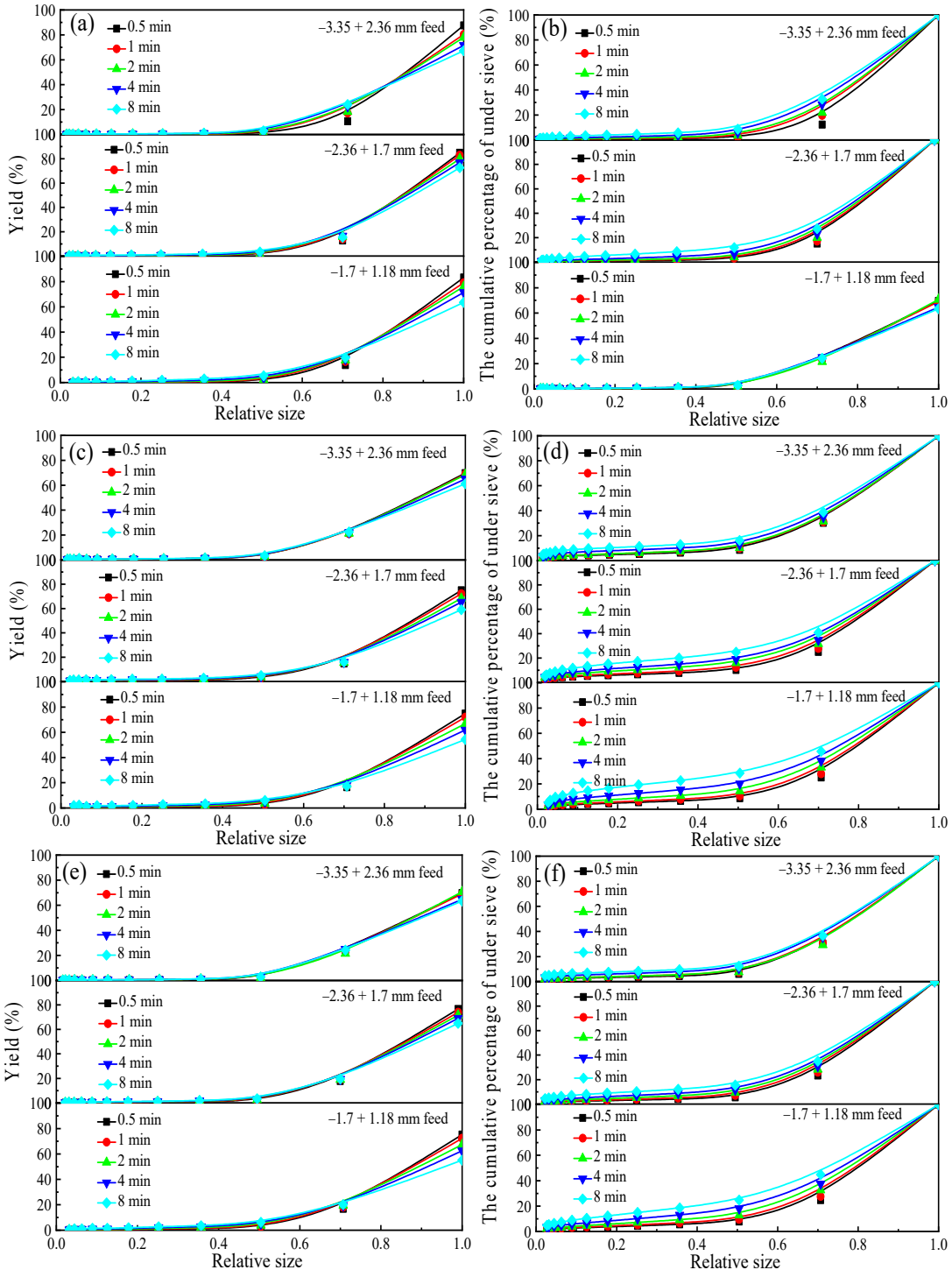

Figure 15. The yield and negative cumulative yield of each product size of three kinds of minerals after grinding: (**a**) yield of quartz, (**b**) cumulative yield under sieve of quartz, (**c**) yield of pyrrhotite, (**d**) cumulative yield under sieve of pyrrhotite, (**e**) yield of pyrite, and (**f**) cumulative yield under sieve of pyrite.

From Figure 15, it can be seen that quartz, pyrrhotite, and pyrite mainly generate adjacent particle sizes of the feed-particle size after grinding, while the yield of other product particle sizes is small. It can be considered that a main crushing mechanism occurs during the grinding process of minerals [37,38]; that is, when the grinding medium

slides, low-strength stress is locally applied to the mineral particles, and the mineral particles undergo wear, causing the fine particles on the surface of the parent particles to fall off, resulting in the formation of small particles with smaller particle sizes and products that are close to the size of the parent particles. The grinding experiments of three minerals have verified this mechanism. It can also be seen from Figure 15 that under the grinding action of 8 min, the three minerals mainly produce particle sizes 0.71 times the feed-particle size, while other particle sizes produce fewer products. Moreover, both the yield curve and the cumulative yield curve under sieve have significant transitions at 0.5 times the feed-particle size. It can be considered that one half of the feed-particle size is the critical particle size for grinding, and very few products smaller than this particle size are generated during the grinding process.

4. Conclusions

(1) From the perspective of particle-size distribution of grinding products, grinding in a cascading state of grinding media mainly involves grinding the feed-particle size into a second coarse particle size. The yield and t_{10} value of other fine particle sizes are very low, and they are mainly composed of newly generated fine particles below −0.038 mm. The particle-size distribution characteristics of grinding products under this test condition are significantly different from those of conventional grinding products. The generation rate of most fine particle sizes in the grinding products under the test conditions conforms to the first-order grinding dynamics characteristics.

(2) The feed-particle size and the hardness of the mineral sample affect the grinding behavior. From the perspective of the product-generation rate of each fine particle size, the smaller the mineral hardness or the smaller the feed-particle size, the greater the generation rate of the fine particle size. The order in which the generation rate of fine particle sizes is compared from the impact of hardness is: pyrrhotite > pyrite > quartz. From the perspective of particle size impact, the order of generation rate of fine particle sizes is: −1.70 + 1.18 mm > −2.36 + 1.7 mm > −3.35 + 2.36 mm. However, from the perspective of the self-breakage rate of the feed-particle size, the breakage rate and its increase rate of various mineral samples are not completely positively correlated with the feed-particle size.

(3) According to the relative feed-particle size, in grinding at different grinding times, the main particle size generated is 0.71 times the feed-particle size, while the other fine particle sizes generated are less than 0.5 times the feed-particle size.

Author Contributions: Conceptualization, J.Y. and S.M.; Data curation, X.Y. and H.L.; Formal analysis, X.D. and W.X.; Funding acquisition, S.M.; Investigation, H.L. and X.Y.; Methodology, J.Y. and S.M.; Project administration, J.Y. and X.Y.; Validation, H.L. and X.Y.; Writing—Original draft, H.L. and J.Y.; Writing—Review and editing, J.Y. and S.M. All authors have read and agreed to the published version of the manuscript.

Funding: This research was funded by the National Natural Science Foundation of China (No. 52274258, No. 51874105).

Data Availability Statement: Not applicable.

Conflicts of Interest: The authors declare no conflicts of interest.

References

1. Park, J.; Kim, K. Use of drilling performance to improve rock-breakage efficiencies: A part of mine-to-mill optimization studies in a hard-rock mine. *Int. J. Min. Sci. Technol.* **2020**, *30*, 179–188.
2. Hashim, S.F.S.; Hussin, H. Effect of grinding aids in cement grinding. *J. Phys. Conf. Ser*. **2018**, *1082*, 012091.
3. Krishnaraj, L.; Ravichandran, P.T. Investigation on grinding impact of fly ash particles and its characterization analysis in cement mortar composites. *Ain Shams Eng. J.* **2019**, *10*, 267–274.
4. Camalan, M. Correlating common breakage modes with impact breakage and ball milling of cement clinker and chromite. *Int. J. Min. Sci. Technol.* **2020**, *30*, 901–908.
5. Chen, B.C. Grinding Principle. *Met. Ind. Press.* **1989**, *1*, 181–252. (In Chinese)

6. Huang, K.Q.; Xiao, C.H.; Wu, Q.M. Application of accurate ball-load-addition method in grinding production of some Tailings. *Adv. Mat. Res*. **2014**, *962*, 771–774.
7. Rabieh, A.; Eksteen, J.; Albijanic, B. Galvanic interaction of grinding media with arsenopyrite and pyrite and its effect on gold cyanide leaching. *Miner. Eng.* **2018**, *116*, 46–55.
8. Peng, Y.; Grano, S. Effect of Iron Contamination from Grinding Media on the Flotation of Sulphide Minerals of Different Particle Size. *Int. J. Miner. Process.* **2010**, *97*, 1–6.
9. Ma, S.J.; Li, H.J.; Shuai, Z.C.; Yang, J.L.; Xu, W.Z.; Deng, X.J. Research on grinding characteristics and comparison of Particle-Size-Composition prediction of rich and poor ores. *Minerals* **2022**, *12*, 1354.
10. Hfels, C.; Dambach, R.; Kwade, A. Geometry Influence on Optimized Operation of a Dry Agitator Bead Mill. *Miner. Eng.* **2021**, *171*, 107050.
11. Santosh, T.; Soni, R.K.; Eswaraiah, C.; Rao, D.S.; Venugopal, R. Optimization of stirred mill parameters for fine grinding of pge bearing chromite Ore. *Particul. Sci. Tec.* **2020**, *39*, 663–675.
12. Yang, J.L.; Shuai, Z.C.; Zhou, W.T.; Ma, S.J. Grinding optimization of cassiterite-polymetallic sulfide ore. *Minerals* **2019**, *9*, 134.
13. Radziszewski, P.; Tarasiewicz, S. Modelling and simulation of ball mill wear. *Wear* **1993**, *160*, 309–316.
14. Ma, S.J.; Li, H.J.; Shuai, Z.C.; Yang, J.L.; Deng, X.J.; Xu, W.Z. Research on grinding law and grinding parameters optimization of polymetallic complex ores. *Minerals* **2022**, *12*, 1283.
15. Zhou, W.T.; Han, Y.X.; Li, Y.J.; Yang, J.L.; Ma, S.J.; Sun, Y.S. Research on prediction model of ore grinding particle size distribution. *J. Disper. Sci. Technol*. **2020**, *41*, 537–546.
16. Owusu, K.B.; Zanin, M.; Skinner, W.; Asamoah, R.K. Ag/sag mill acoustic emissions characterisation under different operating conditions. *Miner. Eng.* **2021**, *171*, 107098.
17. Aldrich, C. Consumption of steel grinding media in mills—A review. *Miner. Eng.* **2013**, *49*, 77–91.
18. Cleary, P.W. Charge behaviour and power consumption in ball mills: Sensitivity to mill operating conditions, liner geometry and charge composition. *Int. J. Miner. Process.* **2001**, *63*, 79–114.
19. Ali, Y.; Garcia-Mendoza, C.D.; Gates, J.D. Effects of 'impact' and abrasive particle size on the performance of white cast irons relative to low-alloy steels in laboratory ball mills. *Wear* **2019**, *426–427*, 83–100.
20. Gates, J.D.; Dargusch, M.S.; Walsh, J.J.; Field, S.L.; Hermand, M.J.P.; Delaup, B.G. Effect of abrasive mineral on alloy performance in the ball mill abrasion test. *Wear* **2008**, *265*, 865–870.
21. Guo, W.; Han, Y.X.; Gao, P.; Li, Y.J.; Tang, Z.D. A study of the grinding of magnetite/limestone mixture in a stirred mill by the attainable region method. *Powder Technol.* **2021**, *389*, 40–47.
22. Aleksandrova, T.; Nadezhda, N.; Anastasia, A.; Artyem, R.; Valentin, K. Selective Disintegration Justification Based on the Mineralogical and Technological Features of the Polymetallic Ores. *Minerals* **2021**, *13*, 851.
23. Aleksandrova, T.; Nikolaeva, N.; Lieberwirth, H.; Aleksandrov, A. Selective desintegration and concentration: Theory and practice. *EDP Sci.* **2018**, *56*, 03001.
24. Hogg, R.; Dynys, A.J.; Cho, H. Fine grinding of aggregated powders. *Powder Technol.* **2002**, *122*, 122–128.
25. Tong, L.B.; Klein, B.; Zanin, M.; Quast, K.; Skinner, W.; Addai-Mensah, J.; Robinson, D. Stirred milling kinetics of siliceous goethitic nickel laterite for selective comminution. *Miner. Eng.* **2013**, *49*, 109–115.
26. Fuerstenau, D.W.; Phatak, P.B.; Kapur, P.C.; Abouzeid, A.Z.M. Simulation of the grinding of coarse/fine (heterogeneous) systems in a ball mill. *Int. J. Miner. Process.* **2011**, *99*, 32–38.
27. Yang, J.L.; Zhu, P.Y.; Li, H.J.; Li, Z.Y.; Huo, X.N.; Ma, S.J. Research on the Relationship between Multi-Component Complex Ore and Its Component Minerals' Grinding Characteristics under Abrasion Force. *Minerals* **2023**, *13*, 6.
28. Zhou, W.T.; Yang, J.L.; Ma, S.J.; Yang, X.J. Study on optimum grinding parameters based on the crushing energy of ball mill. Nonferrous Met. *Miner. Process. Sect.* **2016**, *5*, 62–65. (In Chinese)
29. Leung, K. *An Energy Based Ore Specific Modelfor Autogenous and Semi-Autogenous Grinding*; University of Queensland (JKMRC): Indooroopilly, Australia, 1987.
30. Napier-Munn, T.J. *Mineral Comminution Circuits Their Operation and Optimization*; JKMRC and the University of Queensland Publishing: Indooroopilly, Australia, 2005.
31. Ma, S.J.; Li, H.J.; Yang, X.J.; Xu, W.Z.; Deng, X.J.; Yang, J.L. Study on Impact Crushing Characteristics of Minerals Based on Drop Weight Tests. *Minerals* **2023**, *13*, 632.
32. Zuo, W.R.; Shi, F.G. A t_{10}-based method for evaluation of ore pre-weakening and energy reduction. *Min. Eng.* **2015**, *79*, 212–219.
33. Faramarzi, F.; Napier-Munn, T.; Morrison, R.; Kanchibotla, S.S. The extended drop weight testing approach—What it reveals. *Min. Eng.* **2020**, *157*, 106550.
34. Narayanan, S.S.; Whiten, W.J.; Kanchibotla, S.S. Breakage characteristics for ores for ball mill modelling. *Intl. J. R. Mech. Min. Sci. Geo. Abs.* **1983**, *286*, 31–39.
35. Shi, F.N. A review of the applications of the JK size-dependent breakage model. *Int. J. Miner. Process*. **2016**, *155*, 118–129.
36. Narayanan, S.S.; Whiten, W.J. Determination of comminution characteristics from single-particle breakage tests and its application to ball mill scale up. *Trans. Inst. Min. Metall.* **1988**, *97*, 115–124.

37. Silvana, D.I.; Agnese, M.; Ezio, M. Characterization of particle number and mass size distributions from a small compression ignition engine operating in diesel/methane dual fuel mode. *Fuel* **2016**, *180*, 613–623.
38. Hennart, S.L.; Wildeboer, W.J.; VanHee, P. Identification of the grinding mechanisms and their origin in a stirred ball mill using population balances. *Chem. Eng. Sci.* **2009**, *64*, 4123–4130.